

Structural, physical, and electrical properties of boro-vanadate-iron glasses doped with K_2O alkali

Harshvadan R. PANCHAL*

Department of Chemical and Physical Sciences, University of Toronto Mississauga, Mississauga, Ontario, Canada

Received: 24.06.2013 • Accepted: 14.11.2013 • Published Online: 17.01.2014 • Printed: 14.02.2014

Abstract: The structural, physical, and electrical properties of semiconducting oxide glasses with composition xK_2O : (95-X) $[B_2O_3 : 2V_2O_5] : 5Fe_2O_3$ ($0 \leq x \leq 30$) have been studied. The glasses were prepared by splat-quenching method. Fourier transform infrared spectroscopy (FTIR) studies of these glasses were carried out to study the effect of the modifier and glass former in the glasses. These changes in the molecular structure, bond length, and vibrational group were studied in the spectral range of 400–1350 cm^{-1} . The increase in the intensity and shifting of vibrational bands occurred towards lower wave numbers at 1400–1350 cm^{-1} , 1200 cm^{-1} , and 100–940 cm^{-1} . These structural changes were compared with the electrical conductivity data to see a more clear effect of the glass modifier K_2O in the network formed by glass former V_2O_5 - B_2O_3 . Electrical conductivity of these glasses was studied for all glasses and results were explained on the basis of Mott's theory of conduction mechanism. A decrease in the conductivity with increase of V-V spacing was observed, which was also confirmed by structural changes observed in the FTIR results of these glasses. The present glasses exhibited the structural changes and confirmed the n-type of semiconducting nature with adiabatic hopping due to polarons.

Key words: Electrical conductivity, polaron, activation energy, nonbridging oxygen, adiabatic hopping

1. Introduction

Extensive studies have been carried out on semiconducting oxide glasses containing transition metal oxides for their glass structure and electrical conduction mechanisms [1–5]. These semiconducting glasses have been extensively studied due to their various applications in the fields of electrical switching, memory switching, and optical and cathode materials for making solid-state devices and optical fibers [6–11]. The addition of any transition metal oxide makes glasses semiconducting in nature and electrical conduction is observed due to the hopping of electrons [1,3]. Glasses containing V_2O_5 are semiconducting in nature and exhibit stable switching, whereas V_2O_5 - B_2O_3 glasses are widely used as soldering and molding materials [11]. Recent studies by many researchers have focused on the electrical behavior of these glasses and structure studies using various techniques.

Fourier transform infrared spectroscopy (FTIR) is one of the best tools for looking into the structure of these glasses. Various bonding energies of solids may be found by infrared absorption. Pure vibrational spectra are observed in the range of 400–160 cm^{-1} , whereas separation of the vibrational energy level is larger when observed at high frequencies, i.e. lower wave numbers. Infrared spectroscopies of pure B_2O_3 - V_2O_5 have been

*Correspondence: hr_panchal@yahoo.com

extensively investigated [3,4]. In boro-vanadate glasses, structure, distribution, and interaction between V-O-V and B-O-B polyhedrals play very important roles in electron transport. Effects of nonbridging oxygen during formation of glasses have great impacts on the structure of glasses and electrical conduction process [12]. The electrical conduction in these glasses was also explained on the basis of structure properties and changes in structures that occurred in glasses, which was supported by infrared and physical studies. The present study is focused on the structural, physical, and electrical conductivity of a boro-vanadate-iron glass system containing different amounts of K_2O alkali.

The present study of conduction mechanism was made on a $K_2O: V_2O_5: B_2O_3: Fe_2O_3$ glass system. Fe_2O_3 was added as a Mossbauer probe. In the present paper, electrical properties of an $xK_2O: (95-x) [B_2O_3: 2V_2O_5]: 5Fe_2O_3$ glass system have been examined in the temperature range of 315–435 K and an attempt has been made to elucidate the contribution of K_2O and V_2O_5 to the structure and electrical conduction process in the glasses.

The DC conductivity of transition metal oxide glass was expressed in [1] with the following equation:

$$\sigma = \left[\frac{\vartheta_0 e^2 c (1-c)}{kTR} \right] \exp(-2\alpha R) \exp\left(-\frac{W}{kT}\right), \quad (1)$$

where ν_o is the optical phonon frequency ($\approx 10^{13}$ Hz), e is the electronic charge, c is the mole fraction of the site occupied by the electron, R is the average hopping distance, α is the electron wave function decay constant such that $\exp(-2\alpha R)$ represents an electron overlap integral and hence the probability of tunneling, W is the activation energy, and T is the temperature.

$$\begin{aligned} \text{Note: } W &= W_H + (1/2)W_D \quad \text{for } T > \theta_D/2 \\ &= W_D \quad \quad \quad T < \theta_D/4 \end{aligned} \quad (2)$$

where W_H is the polaron hopping energy, θ_D is the Debye temperature, and W_D is the disordered energy.

The polaron hopping energy W_H is given by:

$$W_H = \frac{e^2}{4\varepsilon_p} \left[\frac{1}{\nu_p} - \frac{1}{R} \right], \quad (3)$$

where $\varepsilon_p = (1/\varepsilon_\alpha - 1/\varepsilon_o)^{-1}$ and ε_o and ε_α are static and high-frequency dielectric constant for the glass, respectively. ν_p is the polaron radius, which is given by [13]:

$$\nu_p = \frac{1}{2} \left(\frac{\pi}{6N} \right)^{1/3}, \quad (4)$$

where N is the number of sites per unit volume.

For a polaron to be small, the polaron radius ν_p should be smaller than the atomic site spacing (V-V spacing) R [1].

For a nonadiabatic hopping process $J < \hbar\omega_o$, where J is the electron transfer integral, and for adiabatic hopping, $J > \hbar\omega_o$. This approximation is given by Holstein [14].

$$J \begin{cases} > \left[\frac{2kT}{\pi} \frac{W_H}{\pi} \right]^{1/4} \left[\frac{\hbar\nu_o}{\pi} \right]^{1/2} & \text{Adiabatic } (>) \\ < & \text{Nonadiabatic } (<) \end{cases} \quad (5)$$

J can be estimated from the difference of the mean value of hopping energy and experimental activation energy W .

2. Experimental

2.1. Sample preparation

Analytical grade chemicals V_2O_5 , H_3BO_3 , K_2CO_3 , and Fe_2O_3 were taken as raw materials, which were weighed in appropriate amounts to prepare glass samples xK_2O :

(95-X) [B_2O_3 : $2V_2O_5$]: $5Fe_2O_3$ ($0 \leq x \leq 30$) in steps of 5 mol%. Weighed amounts were mixed well and transferred to a porcelain crucible, which was maintained for 1 h at $250^\circ C$ to remove the moisture. The temperature of the furnace was then raised to $950^\circ C$ and maintained for 4 h. These melts were then quenched onto a clean copper plate at room temperature and subsequently pressed by another plate to provide a faster quenching rate. The X-ray diffraction analysis showed that quenched samples were amorphous.

2.2. Density measurement

The density of the glass samples was measured at room temperature by displacement method using methanol as the immersion liquid and a single pan balance of 10^{-5} g sensitivity. The density measurements were done to determine the number of metal ions per unit volume (i.e. vanadium ions) in the glasses. The number of transition metal ions was determined by assuming the glass structure as uniform, which helped in calculating the polaron radius [1,2] by knowing the number of atomic sites per unit volume as per Eq. (4).

$$\nu_p = \frac{1}{2} \left(\frac{\pi}{6N} \right)^{1/3}$$

Here, N is the number of sites per unit volume (i.e. V_{total} ions in V_2O_5).

2.3. FTIR measurement

The glass samples were crushed into a fine powder and small amount of glass powder was mixed and ground with a relatively large amount of KBr, which is transparent to IR radiation. Disks for measurement of IR absorption spectra were prepared by pressing a mixture at a pressure of 10–15 t for few minutes under vacuum. The infrared spectra of quenched samples were taken with a PerkinElmer 577 infrared spectrometer in the range of $4000\text{--}400\text{ cm}^{-1}$.

2.4. Electrical conductivity measurement

The samples were cut in the form of rectangular pellets of about 2 mm in thickness. These samples were lapped and polished. Silver paste was painted on the polished rectangular surface of the sample. After polishing, samples were kept at $90^\circ C$ for 90 min to remove moisture and stress from the sample. With the painted silver paste, good ohmic contacts were found. These samples were kept between 2 probes of a sample holder and the cell was kept in a furnace, which was controlled by a mercury contact thermometer (JUMO, Germany) and relay. The electrical conductivity of all the glass samples at different temperatures was measured (315–435 K).

3. Results and discussion

3.1. X-Ray diffraction and density

Among the various characterization techniques, X-ray diffraction plays a very key role in structure characterization. The diffraction patterns were taken from 0° to 70° with a $Cu\alpha$ target. The diffraction pattern showed only big halos with no characterization peak, which illustrates the amorphous nature of all of the prepared glasses (Figure 1).

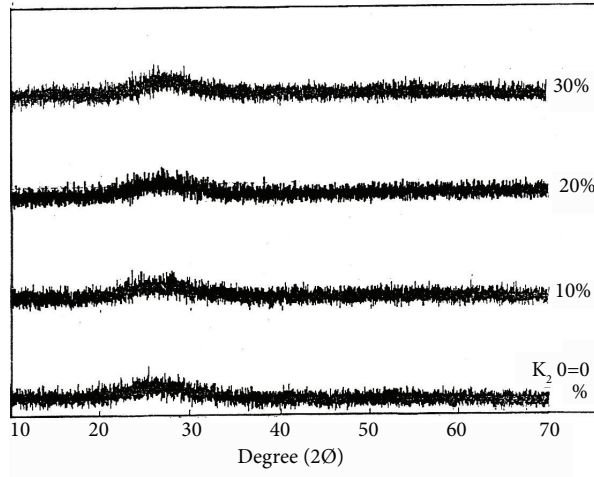


Figure 1. X-ray diffraction pattern of the $x\text{K}_2\text{O}:(95-x)[\text{B}_2\text{O}_3:2\text{V}_2\text{O}_5]:5\text{Fe}_2\text{O}_3$ glass system.

The density of the present glass system was measured using the Archimedes principle. The calculated values of parameters using density measurements are shown in the Table 1, where it can be observed that, as the amount of modifier K_2O is increased, the density of glass samples is also increased. The calculated values of spacing between vanadium atoms (V-V spacing) was found to be increase from 4.16 to 4.52 Å with the content of K_2O . These variations in density and hence V-V spacing help in understanding the electrical conductivity behavior of these glasses.

Table 1. Density, spacing between vanadium (V-V) and boron (B-B), and polaron radius for $x\text{K}_2\text{O}:(95-x)[\text{B}_2\text{O}_3:2\text{V}_2\text{O}_5]:5\text{Fe}_2\text{O}_3$ glass system.

K_2O mol%	Density (g/mL)	ν_P (Å)	W_H (eV)	B-B spacing (Å)	V-V spacing (Å)	Fe-Fe spacing (Å)
0	2.65	1.67	0.327	5.37	4.16	11.33
5	2.71	1.68	0.332	5.54	4.18	11.18
10	2.73	1.70	0.336	5.45	4.22	11.08
15	2.75	1.72	0.339	5.52	4.27	11.00
20	2.77	1.74	0.342	5.60	4.33	10.91
25	2.83	1.76	0.347	5.65	4.37	10.76
30	2.70	1.82	0.343	5.85	4.52	10.86

3.2. FTIR

Figure 2 shows FTIR spectra of pure B_2O_3 , V_2O_5 , and Fe_2O_3 , which are considered for the purpose of comparison. It is seen from the spectrum (line a) in Figure 2 that B_2O_3 has characteristic absorption bands at 1471 cm^{-1} , 1200 cm^{-1} , 780 cm^{-1} , and 653 cm^{-1} . The peaks at 1471 cm^{-1} and 1200 cm^{-1} are assigned to BO_3 triangles [12,13,15]. The peaks at 780 cm^{-1} and 653 cm^{-1} are attributed to bending vibrations of the B-O-B band [15,16]. Figure 2 also shows the FTIR spectrum (line b) of pure V_2O_5 , which has characteristic features at 1020 cm^{-1} , 850 cm^{-1} , and 613 cm^{-1} . The sharp band at 1020 cm^{-1} is assigned to the vanadyl group of the $\text{V}=\text{O}$ bond, whereas 850 cm^{-1} is related to symmetric stretching vibrations along the V-O-V chain involved in corner sharing of the VO_5 polyhedra [16]. A very weak absorption peak at 613 cm^{-1}

corresponds to the V-O-V bond of the symmetrical or bending mode of vibrations. Figure 2 for Fe_2O_3 has the characteristic feature at 563 cm^{-1} attributed to the vibrations of FeO_4 groups of Fe_2O_3 .

The effect of modifier K_2O were studied by keeping V_2O_5 and B_2O_3 at a ratio of 2:1 for fixed amounts of Fe_2O_3 at 5 mol%. The FTIR spectra of all glass samples for $\text{K}_2\text{O} = 0\text{ mol}\%$ to $30\text{ mol}\%$ are given in Figure 3. The main features of these spectra are the appearances of resonance peaks at 1430 cm^{-1} , 1353 cm^{-1} , 1192 cm^{-1} , 1253 cm^{-1} , 1104 cm^{-1} , and $1000\text{--}940\text{ cm}^{-1}$ and very weak broad bands at $804\text{--}602\text{ cm}^{-1}$ and $860\text{--}651\text{ cm}^{-1}$. A close examination of the spectra reveals a very small shift of the vibrational band at 1430 cm^{-1} up to $20\text{ mol}\%$ K_2O . When the amount of K_2O is further increased, the vibrational band at 1430 cm^{-1} splits into 2 vibrations, 1353 cm^{-1} and 1435 cm^{-1} , which are assigned to characteristics of the B-O-B linkage in which both borons are triangularly coordinated or --B--B-- stretching vibrations [15]. The peaks at 1435 cm^{-1} and 1353 cm^{-1} are slightly shifted to 1437 cm^{-1} and 1350 cm^{-1} wavenumbers at $30\text{ mol}\%$ K_2O . In the pure borate glasses, the main structural element is a boroxol ring of plane trigonal configuration with B-O bond length of $1.36 \pm 0.005\text{ \AA}$, whereas the B-O bond length for the BO_4 tetrahedra was $1.47 \pm 0.01\text{ \AA}$. In the spectra, the increase in bond length is seen as the shifting of an absorption band toward the lower wavenumber. In binary borate glasses, up to $14\text{ mol}\%$ K_2O does not break bridging in the BO_3 groups to form BO_4 tetrahedra [15,16]. One K_2O causes the formation of 2 BO_4 tetrahedra, which participate in a 3-dimensional network, thus

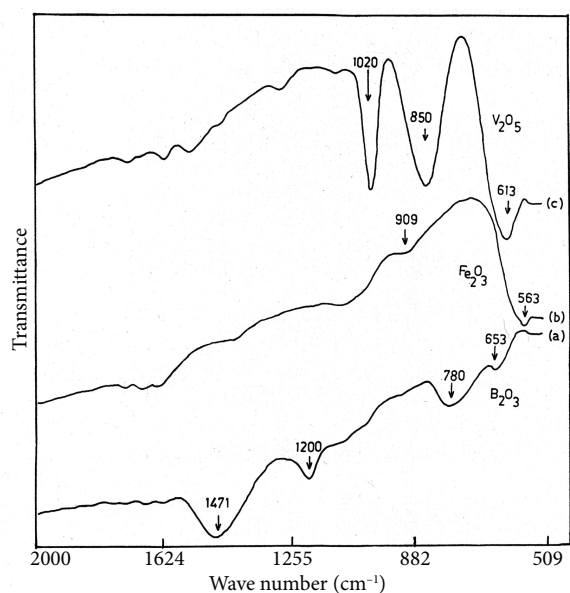


Figure 2. FTIR spectra of pure (a) B_2O_3 , (b) V_2O_5 , and (c) Fe_2O_3 .

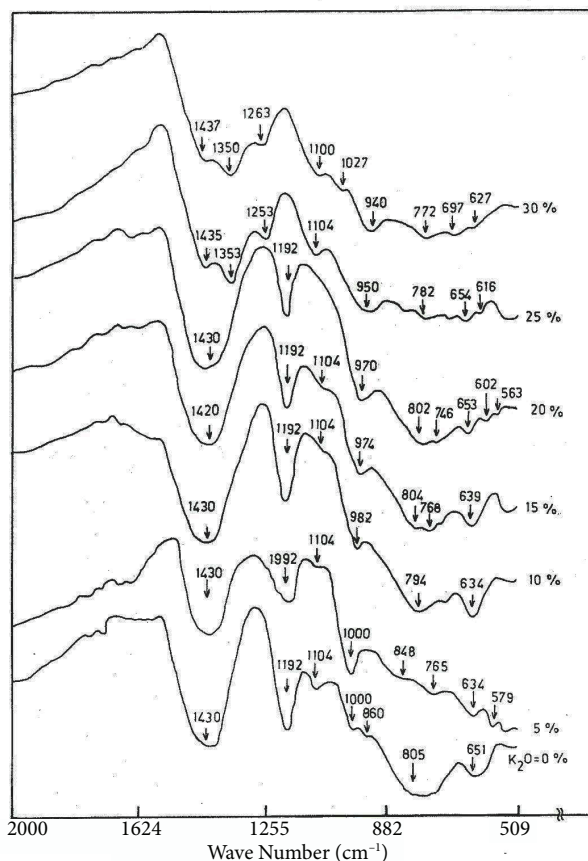


Figure 3. FTIR spectra of $x\text{K}_2\text{O} : (95-x) [\text{B}_2\text{O}_3 : 2\text{V}_2\text{O}_5] : 5\text{Fe}_2\text{O}_3$ glass system for $\text{K}_2\text{O} = 0$ to $30\text{ mol}\%$.

strengthening the structure [17]. The B-O-B separation has been observed to increase, which was calculated from density measurements [15], as shown in Table 1.

Another feature of the IR spectra is the presence of a highly intense peak at 1192 cm^{-1} , which is assigned to BO_3 polyhedra. This peak that disappeared after 20 mol% K_2O shows a presence of a new peak at 1253 cm^{-1} , which is assigned to the $=\text{B-O-B}\equiv$ linkage in which boron is tetrahedrally coordinated [15,16]. For all glass samples from $\text{K}_2\text{O} = 0$ to 30 mol%, a vibrational peak at 1104 cm^{-1} is observed, which is assigned to the vibrations of nonbridging oxygen in the form of $=\text{B-O}^-$ or $\text{B}-\text{O}=\text{B}<\text{O}^-$ [15]. The vibrational bands at $1000\text{--}940\text{ cm}^{-1}$ in the spectra are assigned to the isolated $\text{V}=\text{O}$ double bond of the VO_5 polyhedra with the increase of K_2O . This vibrational band shifting towards the lower wavenumber suggests an increase in bond length of the $\text{V}=\text{O}$ bond. This is due to the fact that the added K_2O goes into the structure at an interstitial position, leaving its oxygen. Now K^+ ions directly interact with the oxygen of the $\text{V}=\text{O}$ bond, thereby weakening the frequency of vibration shifts toward lower wavenumbers. Added K_2O gives rise to the formation of a nonbridging oxygen atom, thereby weakening the $\text{V}=\text{O}$ bond. The presence of a weak and wide absorption band at 860 cm^{-1} and $848\text{--}634\text{ cm}^{-1}$ suggests that it is the sum of the number of absorption bands corresponding to the V-O-V band of slightly varying bond lengths and angles [18-20]. Thus, the formation of nonbridging oxygen results in the increase of distance between V-V atoms, which is also supported by the density measurement data shown in Table 1. This variation of V-V spacing is also supported by the electrical conductivity data, which are explained in Section 3.3.

4. Electrical conductivity

The glass modifier plays a very significant role in the formation of glasses and hence changes the properties of glasses like electrical conductivity, thermal switching, and density. The temperature dependence electrical conductivity of the present glass system has been explained with a theory based on polaron hopping conduction [1]. Dependence of electrical conductivity on the amount of glass modifier has also been studied by many researchers [11,21,22]. In the present glass system, the amount of glass modifier is increased from 0 mol% to 30 mol%, whereas the amount of V_2O_5 is decreasing with a simultaneous decrease of B_2O_3 . The amount of Fe_2O_3 has been kept constant in all glass system. Figure 4 shows the dependence of conductivity on the amount of modifier K_2O . The added K_2O goes into the glass structure by occupying an interstitial position in the $\text{V}_2\text{O}_5\text{-B}_2\text{O}_3$ network. Because of the breaking of the V_2O_5 structure, atomic site spacing between V-V increases. The V-V spacing calculated from the density measurements shows a change from 4.16 to 4.52 Å. The conductivity of the present glass system is also found to increase from 1.59×10^{-5} to $2.04 \times 10^{-7}\Omega^{-1}\text{ cm}^{-1}$ (at $100\text{ }^\circ\text{C}$) with the increase of activation energy from 0.407 to 0.536 eV. A similar type of behavior was also observed and discussed by Devidas et al. [21] and Sanchez et al. [23]. Thus, with the increase of K_2O amount, the atomic site spacing between V-V is found to increase, which directly affects the mobility of a charge carrier. Additionally, $\text{V}^{+4}/\text{V}_{total}$ is observed to be dependent on K_2O amount. Figure 5 shows the plot of $\log\sigma$ (at $100\text{ }^\circ\text{C}$) and activation energy (W) versus V-V spacing. The observed activation energies for all glass samples were found to be slightly higher than the value obtained for other V_2O_5 -based glasses [21,22]. The variations of conductivity are observed in all glasses from 10^{-6} to $10^{-8}\Omega^{-1}\text{ cm}^{-1}$ and $\log\sigma$ versus $10^3/T$ is linear (Figure 6), which shows the semiconducting behavior of the present glass system. The Seebeck measurements were also studied for the present glass system [24,25]. Mori et al. reported $\text{V}_2\text{O}_5\text{-Sb}_2\text{O}_3\text{-TeO}_2$ and $\text{V}_2\text{O}_5\text{-Bi}_2\text{O}_3\text{-TeO}_2$ glasses as n-types of semiconductors [26,27].

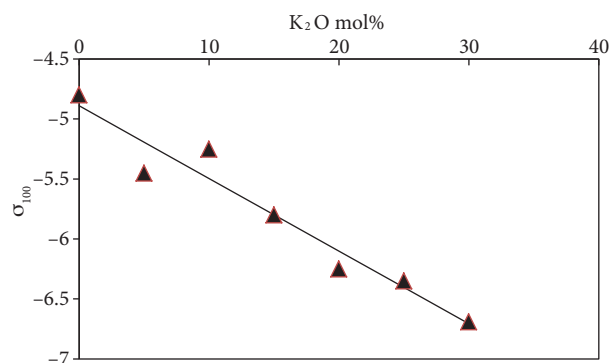


Figure 4. The dependence of conductivity σ_{100} on the amount of modifier K_2O mol%.

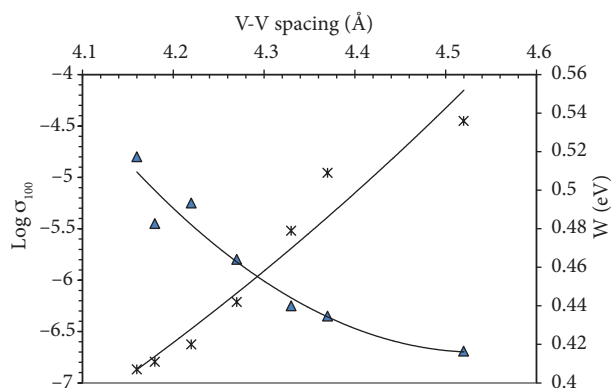


Figure 5. Plot of $\log \sigma$ (at 100 °C) and W (eV) versus V-V spacing.

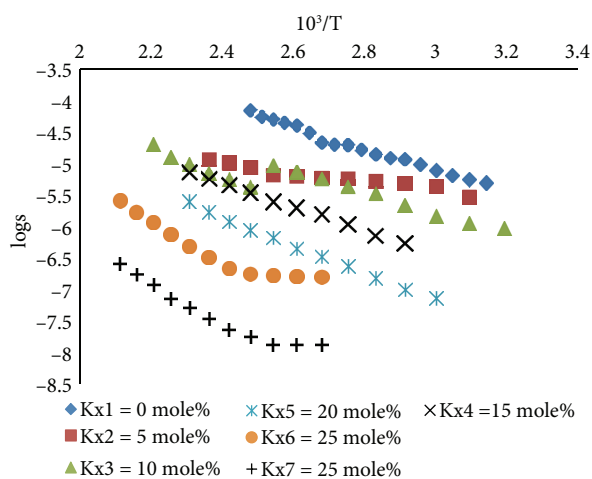


Figure 6. The dependence of conductivity $\log \sigma$ versus $1000/T$ for the $xK_2O: (95-X) [B_2O_3: 2V_2O_5]: 5Fe_2O_3$ glass system.

For a polaron to be small, the polaron radius should be greater than the radius of the iron on which the electron is localized but less than the distance R separating 2 sites. As is evident for the present glass system (Table 2), the value of the polaron radius lies between 1.67 and 1.82 Å, which is less than R , the atomic site separation 4.16–4.52 Å. This satisfies the condition for small polaron hopping. Similar results were also reported for $PbO-P_2O_5-V_2O_5$ glasses [27].

Holstein [14] suggested that the hopping process is controlled by the activation energy and is given by Eq. (5). Calculated values of W_H lie in the range of 0.327–0.343 eV (from Table 2). As per Eq. (5), the values of the right-hand side were calculated for an optical phonon frequency of approximately 10^{13} Hz. The values lie in the range of 0.0124–0.0126 eV. These values are less than the value of J , which lies in the range of 0.0689–0.01973 eV, satisfying the condition for adiabatic hopping in different types of glasses. Hirashima et al. also reported adiabatic hopping in $PbO-P_2O_5-V_2O_5$ glasses [27], as did El-Desoky in $V_2O_5-B_2O_3-BaO$ glasses [28].

Thus, in the present glass system, the effect of the glass modifier plays an important role in the conductivity behavior, which is supported by FTIR and density measurement data. The increase of K_2O

amounts in the glass network modified the structure and led to an increase of V-V spacing, thereby decreasing the conductivity of these glasses. The n-type of the semiconducting nature of the glasses was also confirmed by Seebeck measurements of the present glass system [24,25].

Table 2. Electrical conductivity parameters and other related parameters for $x\text{K}_2\text{O} : (95-x) [\text{B}_2\text{O}_3 : 2\text{V}_2\text{O}_5] : 5\text{Fe}_2\text{O}_3$ glass system.

K_2O mol%	W (eV)	J	$\left(\frac{2kTW_H}{\pi}\right)^{1/2} \left(\frac{h\vartheta_o}{\pi}\right)^{1/2}$ (eV)	σ_{100} ($\Omega^{-1} \text{cm}^{-1}$)	V-V spacing (\AA)	Mobility (μ)
0	0.407	0.0689	0.0124	1.59×10^{-5}	4.16	4.70×10^{-7}
5	0.411	0.0729	0.0125	3.55×10^{-6}	4.18	7.50×10^{-8}
10	0.420	0.0819	0.0125	5.62×10^{-6}	4.22	1.11×10^{-7}
15	0.442	0.1039	0.0126	1.59×10^{-6}	4.27	3.10×10^{-8}
20	0.479	0.1409	0.0126	5.62×10^{-7}	4.33	9.00×10^{-9}
25	0.509	0.1709	0.0126	4.47×10^{-7}	4.37	7.00×10^{-9}
30	0.536	0.1979	0.0126	2.04×10^{-7}	4.52	3.10×10^{-9}

5. Conclusion

The structural and electrical properties of $x\text{K}_2\text{O} : (95-x) [\text{B}_2\text{O}_3 : 2\text{V}_2\text{O}_5] : 5\text{Fe}_2\text{O}_3$ ($0 \leq x \leq 30$) mol% have been studied. The structural changes in these glasses were observed due to the formation of nonbridging oxygen, which was due to formation of BO_4 from the BO_3 group. Spacing between V-V was found to increase as a result of the increase of K_2O content. These results also support the electrical conductivity data. Furthermore, the increase in V-V spacing inhibits the mobility of small polarons as well as the hopping of energy. This results in the decrease of conductivity from 1.59×10^{-5} to $2.04 \times 10^{-7} \Omega^{-1} \text{cm}^{-1}$ (at 100°C) and the increase of activation energy from 0.407 to 0.536 eV. This change is also confirmed from the IR spectroscopy measurement of the present glass system. The present glass system confirmed that the n-type of semiconducting nature and conduction is due to polaron hopping, which is adiabatic in nature.

References

- [1] Mott, N. F. *J. Non-cryst. Solids* **1968**, *1*, 1–17.
- [2] Al-Hajry, A.; Al-Shahrani, A.; El-Desly, M. M. *Mater. Chem. Phys.* **2006**, *95*, 300–306.
- [3] Sindhu, S.; Sanghi, S.; Agarwal, S. A.; Seth, V. P.; Kishore, N. *Physica B* **2005**, *365*, 65–75.
- [4] Sen, S.; Ghosh, A. *J. Non-cryst. Solids* **1999**, *258*, 29–33.
- [5] Austin, I. G.; Mott, N. F. *Adv. Phys.* **1969**, *18*, 71, 41–102.
- [6] Darke, C. F.; Scanlan, L. F.; Enege, A. *Phys. Status Solidi* **1969**, *32*, 193. Mansingh, A.; Singh, R.; Krupanidhi, S. B. *Solid State Electron.* **1980**, *23*, 649–654.
- [7] Montani, R. A.; Levy, M. J.; Souquet, L. *J. Non-cryst. Solids* **1992**, *149*, 249–156.
- [8] Panchal, H. R.; Kanchan, D. K. *Turk. J. Phys.* **1999**, *23*, 969–976.
- [9] Mekki, A.; Khattak, G. D; Siddiqui, M. N. *Int. J. Mod. Phys. B* **2010**, *24*, 1471–1488.
- [10] Wozniak, I.; James, P. F. *Glass Technol.* **1984**, *25*, 98–104.
- [11] Sanad, A. M.; Kashif, I.; El-Sharkawy, A. A.; El-Saghir, A. A.; Farouk, H. J. *Mater. Sci.* **1986**, *21*, 3490.
- [12] Kashif, I.; Farouk, H.; Aly, A. S.; Sanad, A. M. *Phys. Chem. Glasses* **1991**, *32*, 77–78.

- [13] Holstein, T. *Ann. Phys.* **1959**, *8*, 34.
- [14] Li, H.; Lin, H.; Chen, W.; Luo, L. *J. Non-cryst. Solids* **2006**, *352*, 3069–3073.
- [15] Kanchan, K.; Panchal, H. *Turk. J. Phys.* **1998**, *22*, 989–996.
- [16] Bratu, I.; Oana, P.; Culea, M. *Phys. Status Solidi A* **1987**, *100*, K195–K198.
- [17] Bachmann, H. G.; Ahmed, F. R.; Barnes, W. H. *Z. Kristallogr.* **1961**, *115*, 110–131.
- [18] Assem, E.; Elmehasseb, I. *J. Mater. Sci.* **2011**, *46*, 7, 2071–2076.
- [19] Kim, Y. Y.; Kim, K. H.; Choi, J. S. *J. Phys. Chem. Solid* **1989**, *50*, 903–908.
- [20] Devidas, G. B.; Sankarappa, T.; Chougule, B. K.; Prasad, G. *J. Non-cryst. Solids* **2007**, *353*, 426–434.
- [21] Dixit, V. G.; Singh, K. *J. Phys. Chem. Solids* **1983**, *44*, 859–864.
- [22] Sanchez, C.; Linage, J. *J. Non-cryst. Solids* **1984**, *65*, 285–300.
- [23] Panchal, H. R.; Kanchan, D. K. In *Proceedings of the DAE Solid State Physics Symposium*, University of Kurukshetra, Kurukshetra, India, 27–31 December 1998; Mukopadhyay, R. K.; Saikh, A. M.; Godwal, B. K., Eds.; Hyderguda, Hyderabad, India: Universities Press (India) Limited, **1999**, p. 256–257.
- [24] Panchal, H. R. PhD, Department of Physics, The Maharaja Sayajirao University of Baroda, Gujarat, India, 2000.
- [25] Mori, H.; Sakata, H. *J. Mater. Sci. (UK)* **1996**, *31*, 1621.
- [26] Hirashima, H.; Nishi, K.; Yoshida, T. *J. Am. Ceram. Soc.* **1985**, *68*, 486–489.
- [27] El-Desoky, M. M. *Phys. Status Solidi A* **2003**, *195*, 422–428.